

# The global pyrogeography of ecoregion flammability thresholds

Todd Ellis<sup>1</sup>, David Bowman<sup>1</sup>, and Grant Williamson<sup>1</sup>

<sup>1</sup>University of Tasmania

September 27, 2023

## Abstract

Anthropogenic climate change is creating a more flammable future by increasing the number of days when vegetation is dry enough to burn. Indices representing the percent moisture content of dead fine fuels as derived from meteorological data have been used to assess geographic patterns and temporal trends in vegetation flammability. To date, this approach has assumed a single flammability threshold, typically between 8 and 12%, controlling fire potential regardless of the vegetation type or climate domain. Here we investigate geographic variation in fuel moisture levels associated with observed fire activity among ecoregions by analysing global reanalysis data and remotely sensed burnt area products. This geospatial analysis identified a wide range of ecoregion flammability thresholds (EFTs) associated with fire activity, often well above or below the commonly used range of values. Many boreal and temperate forests, for example, can burn with much higher fuel moisture than previously identified; Mediterranean forests, on the other hand, tend to burn with consistently low fuel moisture. Bayesian modelling showed that EFTs are primarily driven by eco-climatological variables, particularly precipitation and temperature. Our analysis also identified complex associations between vegetation structure, fuel types, and climatic conditions highlighting the complexity in vegetation-climate-fire relationships globally. Our study provides a critical, necessary step in understanding and describing global pyrogeography and tracking changes in spatiotemporal fire activity.

The global pyrogeography of ecoregion flammability thresholds

**Abstract.** Anthropogenic climate change is creating a more flammable future by increasing the number of days when vegetation is dry enough to burn. Indices representing the percent moisture content of dead fine fuels as derived from meteorological data have been used to assess geographic patterns and temporal trends in vegetation flammability. To date, this approach has assumed a single flammability threshold, typically between 8 and 12%, controlling fire potential regardless of the vegetation type or climate domain. Here we investigate geographic variation in fuel moisture levels associated with observed fire activity among ecoregions by analysing global reanalysis data and remotely sensed burnt area products. This geospatial analysis identified a wide range of ecoregion flammability thresholds (EFTs) associated with fire activity, often well above or below the commonly used range of values. Many boreal and temperate forests, for example, can burn with much higher fuel moisture than previously identified; Mediterranean forests, on the other hand, tend to burn with consistently low fuel moisture. Bayesian modelling showed that EFTs are primarily driven by eco-climatological variables, particularly precipitation and temperature. Our analysis also identified complex associations between vegetation structure, fuel types, and climatic conditions highlighting the complexity in vegetation-climate-fire relationships globally. Our study provides a critical, necessary step in understanding and describing global pyrogeography and tracking changes in spatiotemporal fire activity.

## 1 Introduction

There is growing consensus that anthropogenic climate change is causing longer and more intense fire seasons (Balch et al., 2022; Ellis et al., 2022; Jain et al., 2022), with a corresponding increase in the number of

wildfires exhibiting extreme behaviour with adverse socio-ecological and -economic impacts (Bowman et al., 2017; Duane et al., 2021). Climate projections suggest this trend is likely to continue throughout the 21<sup>st</sup> century (Flannigan et al., 2013; Wotton et al., 2017; Abatzoglou et al., 2019; Abatzoglou et al., 2021). Western North American forests, for example, have shown a rapid increase in annual burnt area in the last half century (Westerling, 2016; Williams et al., 2019) – albeit this trend is partially driven by a long history of deleterious land-use practices such as fire suppression (Abatzoglou et al., 2018). Current climatological and ecological modelling suggests the occurrence of catastrophic megafire events in the USA, such as those seen in the 2020 fire season (Higuera and Abatzoglou, 2020), will continue to increase across affected forests due to anthropogenic climate change (Bowman et al., 2020). The potential severity of these events, however, may be reduced by fuel management intervention that restores pre-colonial fire regimes (Abatzoglou et al., 2021; Hessburg et al., 2021). A similar increase in extreme fires is also evident in southeastern Australia (Sharples et al., 2016; Abram et al., 2021), where trends in both drought and extreme fire weather combined with the loss of Indigenous fire management are believed to have contributed to the catastrophic 2019 – 2020 fire season dubbed the Australian Black Summer (Boer et al., 2020; Nolan et al., 2020; Canadell et al., 2021; Collins et al., 2021; van Oldenborgh et al., 2021; Mariani et al., 2022).

The fuel moisture content of live and dead fine fuels is inherently linked to the behavioural and ignition determinants of wildfire driving these trends across multiple spatial and temporal scales (Bradstock, 2010; Murphy et al., 2013). Dead fine fuel moisture content (DFFMC) has specifically been identified as a key switch determining the spread of vegetation fire. Dead surface fuels such as leaves, bark, twigs, and grass are capable of rapidly equilibrating with atmospheric humidity in under 10 hours, and consequently represent the most ignitable component of vegetation. As the ignition of these fuels can then provide the energy to ignite both larger dead fuel components and live fuels, DFFMC is therefore a key determinant of overall wildfire occurrence, behaviour, and greater pyrogeographic patterns. To track DFFMC and associated potential fire danger, DFFMC can be measured directly in the field (e.g. Bowman et al., 2020) or estimated using meteorological indices such as vapour pressure deficit (VPD) or the Canadian Fire Weather Index system (FWI: Van Wagner, 1987). Accordingly, derived or measured DFFMC functions as a prominent proxy for an ecoregion’s potential to ignite and sustain wildfire, accurately reflecting the surface litter most prone to ignition and fire spread (Murphy et al., 2013; Flannigan et al., 2016; Kelley et al., 2019). DFFMC is also of fundamental importance in shaping spatiotemporal patterns of landscape fires from local to global scales. For example, moisture differences are understood to control the spread of fires across different vegetation types such as savannas and rainforests (Little et al., 2012).

Prior research has identified specific values of DFFMC as marking the upper and lower bounds of wildfire potential (Fernandes et al., 2008; Wotton, 2008; Slijepcevic et al., 2015; Flannigan et al., 2016; Nolan et al., 2016; Boer et al., 2017; Filkov et al., 2019; Clarke et al., 2022). For instance, FWI- or VPD-derived DFFMC values of between 8 and 12% have been linked to uncontrollable wildfire (Slijepcevic et al., 2015; Flannigan et al., 2016; Nolan et al., 2016; Boer et al., 2017; Filkov et al., 2019), while values of up to 30% have been found to represent the upper limits of vegetation fire (Fernandes et al., 2008; Nolan et al., 2016) under current atmospheric oxygen concentrations due to carbon fibre saturation (Luke and McArthur, 1978; Scott and Glasspool, 2006).

Global and regional studies frequently estimate DFFMC within the Canadian FWI system due to its ease of calculation and interpretation (Field, 2020); these studies have often applied single value thresholds to assess patterns and likely trends in global fire potential. For instance, an established 10% threshold (Wotton, 2008; Flannigan et al., 2016) was used to infer that the proportion of fire seasons falling below this critical threshold had significantly increased between 1979 and 2019 for most ecoregions worldwide (Ellis et al., 2022). Such a shift is likely to affect established fire regimes, particularly for more productive or wet ecoregions.

There are, however, inherent problems with applying single-value thresholds like this to compare different vegetation types and climate domains. Forest ecosystems have evolved with fire differently in response to naturally occurring environmental and biological constraints like soil fertility, climate, and the local biota. It is thus unlikely that a single DFFMC value could possibly reflect the critical point of flammability across

grossly different ecoregions. Furthermore, fire danger indices are developed for specific, regional forest types, with the FWI having been developed based on a mature *Pinus banksiana* Lamb. and *Pinus contorta* landscape in southern Canada (Van Wagner, 1987; Wotton, 2008). Despite the FWI's established global applicability, there is no reason to assume that the vegetation in these forests is globally representative, and its use may consequently be inappropriate for assessing fire potential or true fuel moisture in different vegetation types (e.g., Aguado et al., 2007; Wotton and Beverly, 2007; Schunk et al., 2017). This raises a question about how fire weather indices can best be used to retain local relevance by identifying ecoregion-specific thresholds controlling the switch from a non-flammable to a flammable state (e.g, Clarke et al., 2022).

Building on these studies, we seek to answer the question of whether a universal fuel moisture threshold exists as a control on fire, while advancing our understanding of how fuel moisture acts as a switch for landscape fire both regionally and globally. Using a comprehensive dataset of over 700 hierarchically defined ecoregions, we identify the ecoregion flammability thresholds (EFTs) as the FWI-derived DFFMC value most associated with rapid step changes in remotely sensed fire activity records. Our methods (Figure 1) bypass the issues inherent with applying fire weather indices globally by localising the relationship between DFFMC and fire to each individual ecoregion with associated satellite fire records. We then use a combination of nonmetric multidimensional scaling and inferential statistical modelling to verify the veracity of EFTs as a biological, localised mechanism and examine both the biogeographic and climate characteristics constraining our identified EFTs as critical fuel-fire switches.

## 2 Materials and methods

### 2.1 Geospatial classification

We used the Terrestrial Ecosystems of the World regional classification system hosted by the World Wildlife Fund (Olson et al., 2001; see supporting information). This dataset groups regions into a hierarchical system using eight realms at the coarsest level (e.g., the Indo-Malay Archipelago and associated lands in Southeast Asia), 14 biomes (e.g., temperate broadleaf and mixed forests), and, at the finest scale, 867 distinct ecoregions (e.g., Madagascar's subhumid forest). These ecoregions represent distinct biota and potential habitats, but do not consider the real effects of human land-use practices such as agricultural clearing. We removed a total of 95 of the 867 original ecoregions from our analyses, including 76 ecoregions with no associated fire records (e.g., those existing in the Antarctic realm). In addition, we removed the mangroves biome type from all analyses, as this biome is comprised of only 19 small, discontinuous ecoregions with fire histories primarily driven by neighbouring biome types.

### 2.2 Identifying and assessing the ecoregion flammability threshold

We used estimated dead fine fuel moisture content (DFFMC: %) as drawn from the Canadian Fire Weather Index (FWI) system's fine fuel moisture conde (Van Wagner, 1987) as a foundation for identifying ecoregion flammability thresholds (EFTs). We chose this estimation of DFFMC due to its established global applicability and ease of both calculation and interpretation (Wotton, 2008; Field, 2020). To calculate DFFMC using the FWI, we used the European Centre for Medium-Range Weather Forecast's ERA5 atmospheric reanalysis data (Hersbach et al., 2020) due to its accessibility and worldwide coverage. It should be recognised that the current ERA5 reanalysis product holds regional biases in capturing observed moisture primarily within the tropics (Lavers et al., 2022). These data were used to calculate daily DFFMC representing noon local standard time between 1979 and 2019 at a gridded 0.25° spatial resolution. High-latitude overwintering periods were removed from the records to reduce the false identification of dry winter periods as highly flammable (McElhinny et al., 2020). See Figure 1 for a detailed workflow diagram.

To then identify each EFT controlling an ecoregion's average ability to ignite and sustain a wildfire, we first calculated the cumulative proportion of burnt area from the Moderate Resolution Imaging Spectroradiometer

(MODIS) MCD64CMQ product (2001 - 2021: Giglio et al., 2018) over the full range of potential EFTs by ecoregion. We constrained the upper bounds of potential EFTs to 70% DFFMC to allow for a safe degree of uncertainty above the known limits of the fibre saturation point (Fernandes et al., 2008). We then used a nonlinear least squares regression formula to fit a logistic curve to the relationship between the cumulative proportion of burnt area (BA) and the upper limit of the ecoregion’s driest DFFMC quartile using Eq. (1). This equation assumes the 25<sup>th</sup> percentile of an ecoregion’s monthly DFFMC is reflective of that ecoregion’s driest period – even where concrete seasonal climate patterns are more nebulous:

$$P(BA < DFFMC) = \frac{\phi_1}{1 + e^{-\frac{\phi_2 - DFFMC}{\phi_3}}}, \quad (1)$$

where  $\phi_1$ ,  $\phi_2$ , and  $\phi_3$  are the asymptote, curve inflection point, and scale parameter of the curve, respectively. We extracted  $\phi_2$  from the model formulae as the inflection point where the greatest marginal increase in the cumulative proportion of burnt area occurred for a given reduction in DFFMC. The DFFMC value at  $\phi_2$  is subsequently the EFT constraining fire potential for a given ecoregion. We also extracted the reciprocal of the model parameter  $\phi_3$ , which provides a proxy measure of the inflection point slope estimate (IPSE). The IPSE complements the EFT and provides insight into the strength of the relationship between DFFMC and fire activity in moisture-limited environments. A total of 74 ecoregions did not have associated fire data within the DFFMC constraints to support identifying an EFT or the associated IPSE. Instead of removing these ecoregions from our analyses, we chose to impute the missing values of those 74 ecoregions using the median EFT from the same hierarchical realm and biome classifications where available. For example, these 74 ecoregions include three boreal forests in either in the Nearctic or Palearctic realms. The two ecoregions in the Nearctic realm were imputed using the median EFT for Nearctic boreal forests (i.e., 14%), while the third from the Palearctic realm was imputed using the median EFT for Palearctic boreal forests (i.e., 16.3%). See supporting information all modelled ecoregional  $P(BA < DFFMC)$  curves as well as biome-level means.

We assessed the identified EFTs by first visualizing the EFT distributions by biome type, highlighting the median and quantile-based intervals. We statistically confirmed the apparent effects of median biome differences using a Kruskal-Wallis rank sum test (Kruskal and Wallis, 1952), and then identified the mean rank differences between specific biome types using a two-way Dunn’s test for pairwise multiple comparisons (Dunn, 1961). We extracted non-significant differences between biome types, highlighting the similarities in fuel-fire relationships dependent on the underlying biota and potential habitats.

### 2.3 Statistical analyses of the fuel moisture-fire relationships

To identify the eco-climatological factors driving the ecoregions’ EFTs, we used a combination of nonmetric multidimensional scaling (NMDS) and generalised additive modelling. This combination of variable ordination and inferential modelling provides a foundation to analyse biogeographic implications of EFTs across different ecoregions and vegetation types. First, we applied NMDS ordination to a suite of climatological and ecological data with known associations to wildfire ignition or spread and then plotted the final ordination against our identified EFTs. We used bioclimatic indicator means (1979 – 2018) for annual precipitation (BIO12:  $\text{m s}^{-1}$ ), annual temperature (BIO01: K), and precipitation seasonality (BIO15: %) from the ERA5 reanalysis dataset available via the Copernicus Climate Data Store (Hersbach et al., 2020; Wouters et al., 2021). We also used a combination of three additional MODIS products: Mean annual net primary productivity (NPP:  $\text{t C ha}^{-1} \text{ year}^{-1}$ ) calculated between 2000 and 2015 (MOD17A3: Running et al., 2015), and two vegetation continuous fields representing the median percent of an ecoregion represented by both herbaceous and tree vegetation in 2020 (MOD44B: DiMiceli et al., 2015). This minimal set of variables were selected as they are commonly applied and have known relationships with fire activity. We tested both two- and three-dimensional nonmetric multidimensional scaling NMDS ordination based on exploratory stress scree and Shepard plotting, ultimately choosing the two-dimensional ordination with a stress index of 0.125 for simplicity. See supporting information for the exploratory NMDS diagnostics behind this rationale. The new, reduced NMDS dimensions were plotted using scatterplot variable ordination with the underlying distribution of EFTs to both explore the effects the different eco-climatological variables theoretically hold, as

well as reduce the number of variables retained in the model.

Building off of the previously-identified association between intermediate productivity and fire activity (Pausas and Bradstock, 2007; Pausas and Ribeiro, 2013; Bowman et al., 2014; Ellis et al., 2022), we plotted global NPP as a function of mean fire activity underlain by both our identified EFTs and the associated IPSEs. This analysis uses 0.25° ERA5 grid cells for NPP and indexed fire activity as shown in Ellis et al. (2022), adding weight to the breadth and extent of both globally. Following those prior analyses, we calculated fire activity indices (FAI: Pausas and Ribeiro, 2013) using the mean annual (2002 – 2020) number of fire detections as recorded in the MODIS active fire database (MCD14DL: Giglio et al., 2003) while excluding permanent, anthropogenic heat sources. By showing both the identified EFT and its associated slope estimate, we highlight the global distribution of EFTs and its relationship with productivity and indexed fire activity, while the IPSE provides insight into the strength of the EFT as a constraint in a particular ecoregion.

Our use of generalised additive modelling employed a Bayesian framework to measure the effects relevant eco-climatological variables have in shaping EFTs. Our modelling focus is ultimately not guided by predictive power, but rather to verify the identified EFTs as a functioning, biological mechanism on ecoregion-level fire behaviour. Because our EFTs can naturally be interpreted as a percentage with a strong positive skew, we estimated the response likelihood function on a beta distribution. Note that while the Canadian FWI’s calculation of DFFMC can reach limits of up to 250%, our EFTs all fall under 100% due to the 70% constraint we applied during our identification of the EFTs. Additionally, it’s unlikely any potential EFT could extend above that maximum based on vegetation’s theoretical maximum fibre saturation point of 30% (Fernandes et al., 2008). Informed by our exploratory analysis of the EFTs and the NMDS ordination, we retained precipitation, temperature, precipitation seasonality, and herbaceous vegetation cover as fixed continuous effects in the model. Of the highly colinear variables, we chose annual precipitation over both NPP and percent tree cover due to the former’s reliance on precipitation, and the latter being inherently linked to herbaceous cover. As realm and biome type don’t reflect true vegetation, but rather a complex, overlapping network of theoretical habitats, we retained both realm and biome only as interactive random effects. See supporting information for additional model development details, including data preparation steps and specific model parameters.

Finally, to evaluate and explain our model within our inferential framework, we focused on a combination of variable importance using permuted *RMSE* dropout loss and Bayesian effects probability measures. First, we calculated the influence of individual variables in the model by using sampled ( $n = 1,000$ ) change in the *RMSE* loss function over 100 permutations. We then evaluated the continuous fixed effects of our model using the sequential effect existence and significance testing framework. This framework succinctly describes the effects of model parameters, providing three interlinked probability measures of overall effect direction (i.e., existence), practical effect significance, and size (i.e., strength) while also being easy to interpret due to the rough equivalence to statistical significance (e.g.,  $p < 0.05$  or a probability greater than 95%). These statistical and visual tools work well in conjunction to describe the impacts of individual eco-climatological variables on effecting the identified EFTs while confirming the complexity of fuel moisture as a biological constraint on localised (i.e., ecoregion-level) fire behaviour.

## 3 Results

### 3.1 Global and biome distributions of ecoregion flammability thresholds

Ecoregion flammability thresholds (EFTs) were identified for 772 of the 867 ecoregions classified in the Terrestrial Ecosystems of the World dataset (Olson et al., 2001), representing a total area of 128.5 M km<sup>2</sup> – about 87% – of the Earth’s terrestrial surface (Figures 2a and 3). The global mean EFT identified was 12.2%, with a median of 11.5%, and an interquartile range of 6.92%. Only 17 ecoregions representing 0.8 M km<sup>2</sup> reported thresholds over the expected maximum of 30%; most of these, however, are likely due to the

limitation of fuel moisture playing a smaller role in the importance of fire for that ecoregion, or artifacts associated with insufficient fire data. The inflection point slope estimates (IPSEs) extracted from the  $P(BA < DFFMC)$  models shows the strongest relationship between DFFMC and burnt area appears to be primarily in different types of desert, tropical and subtropical savannas, higher-latitude forests, and some select tundra environments (Figure 2b).

Across biomes, the lowest identified EFTs were associated with types of shrublands, woodlands, and savanna biomes (Figure 3). The highest identified EFTs, on the other hand, tended to represent higher-latitude forests, as well as tundra. The average wetter temperate and tropical forested biomes closely followed these high-latitude biomes, but also tended to hold the widest range of EFTs, suggesting more complex geospatial relationships between fire, fuel moisture, and anthropogenic stressors. The Kruskal-Wallis rank sum test for differences in EFTs between biome types was strongly significant ( $p < 0.001$ ), while the pairwise multiple comparison statistics calculated using Dunn’s test highlight like and unlike biome types. The statistical grouping of biomes with similar EFTs shows a clear gradient across climate, productivity, and vegetation types, albeit with a wide intra-biome variability associated with the complexity of ecoregions within biomes (Figure 3). See supporting information for pairwise multiple comparison statistics, as well as EFT summary statistics across both biome type and all existing hierarchical realm and biome classifications.

### 3.2 Climatic controls on ecoregion flammability thresholds

The two-dimensional nonmetric multidimensional scaling (NMDS) ordination reveals the role of climatological factors in effecting the identified EFT across the different biome types (Figures 4a-b). The first dimension is primarily driven by precipitation and associated proxies: Higher annual precipitation, net primary productivity (NPP), and more tree cover are interlinked, influencing fuel-fire relationships in moisture-limited or -driven ecoregions. The second scaled dimension is driven primarily and negatively by temperature and is strongly linked to moisture-limited ecoregions with lower EFTs. Precipitation seasonality has a negative effect across both the first and second scaled dimensions, with higher values of precipitation seasonality representing stronger seasonal dryness (e.g., deserts and savannas with arid summer conditions). Similarly, higher herbaceous vegetation cover is associated with cooler, drier ecoregions. Outside of higher-latitude tundra and forest types, Earth’s biome types on average hold lower EFTs driven by temperature and precipitation on the second NMDS axis (Figure 4b).

The average EFT is well below the expected 30% limit for carbon fibre saturation across the full range of the productivity–fire activity index gradient (Figure 5a), noting that the majority of the Earth’s ecoregions by areas have a NPP below  $10 \text{ t C ha}^{-1}\text{year}^{-1}$  (Figure 5b). Within the intermediate NPP range (i.e., roughly  $1.2 - 5.4 \text{ t C ha}^{-1}\text{year}^{-1}$  per year for the evaluated ecoregions) where fire activity indices are maximal, EFTs are moderately higher than on either side of this productivity range or in those ecoregions with less fire activity. The lowest EFTs occur within the least productive environments across the entire range of fire activity. Low EFTs also occur to the right of the intermediate NPP range within those ecoregions that are frequently burnt. Both these areas of extremely low EFTs also tend to have the sharpest associated IPSEs (Figure 5c). There ultimately exists strong relationships between DFFMC and burnt area across most of the Earth’s ecoregions, apart from those highly productive, wet tropical forests, (Figure 5b).

Our application of generalized additive modelling of EFT against environmental predictors showed a strong effect of the three bioclimatic indicators, with less explanatory power for biogeographic and ecological variables. This final model reported a correlation coefficient of determination ( $R^2$ ) of 0.682 and a root-mean-square error ( $RMSE$ ) of 0.038 for the complete distribution of EFTs. See supporting information for comparable statistics for training, testing, and cross-validation datasets. Our analysis of variable importance shows that  $RMSE$  dropout loss was sensible between predictor variables (supporting information). The three nonlinear bioclimatic indicators representing mean annual precipitation, mean annual temperature, and mean precipitation seasonality report the greatest influence on the model’s accuracy, followed distantly by the terrestrial realm and biome classifications as random effects. Median percent herbaceous cover reported a consistent, negligible effect on the model  $RMSE$  loss. The effects statistics confirm this, showing that precipitation is

the strongest predictor of the global EFT distribution. In contrast to the variable importance analysis, the effect of precipitation seasonality on EFTs is larger and more significant than temperature (Table 1). See supporting information for model evaluation steps including conditional effects and both the predicted and expected posterior distributions.

## 4 Discussion

Ecoregions within a given biome have similar fuel moisture thresholds (EFT) associated with observed landscape fires (Figures 1, 3). There is, however, significant variability in the biogeography of EFTs (Figures 2a, 3), which suggests that a single fuel moisture threshold cannot be interpreted as a universal determinant of flammability. This global variability is sensibly explained by eco-climatological variables like precipitation and temperature. In addition to contextualizing the EFTs in relation to these eco-climatological variables, they need to be considered in concert with the inflection point slope estimates (IPSEs) and fire activity as outlined below. These considerations are important in understanding the likely effects of climate change on fire regimes, as well as determining those ecoregions and biomes where the risk of fire activity is increasing. We propose identification and use of these EFTs is critical to understanding the future of global pyrogeography.

### 4.1 The biogeography of flammability thresholds

The global averages for our EFTs correspond closely to the extreme values of between 8 and 12% identified or used in prior research (Wotton, 2008; Slijepcevic et al., 2015; Flannigan et al., 2016; Nolan et al., 2016; Boer et al., 2017; Filkov et al., 2019; Ellis et al., 2022). This suggests that those commonly used EFTs as derived from the Canadian FWI system and ERA5 reanalysis data do, on average, reflect ecological switches controlling fire ignition and spread for many Earth environments. Despite this, relying on a global average oversimplifies local fuel-fire relationships and ignores our understanding of how the fibre saturation point can vary between landscapes and vegetation types (Fernandes et al., 2008; Alvarado et al., 2019). Biome-level differences in EFTs suggest that a generalized threshold will often under- or over-estimate the localised fuel moisture-fire relationship, with nearly 70% of the Earth’s surface holding an EFT above or below that range of 8 and 12%. The geographic distribution of EFTs (Figure 2a) as well as the differences between and within distinct biome EFT distributions (Figure 3) highlight where this oversimplification fails to capture the true association between fuel moisture and fire. This includes, for instance, all boreal forests (Q1: 13.9%, Q3: 16.6%) and tundra (Q1: 17.7%, Q3: 19.8%) ecoregions, as well as those North American *Pinus banksiana* and *Pinus contorta* forests where the FWI system originates (Van Wagner, 1987). For ecoregions or biomes such as these, the general threshold grossly under-estimates the true fuel moisture content shown to be associated with fire (Figure 3).

The need for biogeographically-variable EFTs is logical given the role water availability – including the moisture content of both live and dead fuels – plays in fuel accumulation within different types of fire regimes (Murphy et al., 2013). A universal threshold oversimplifies the distinct biology of vegetation and how vegetation in different ecoregions may have evolved with fire. A bespoke threshold can more accurately capture the existing variation in live and dead fuel moisture content associated with the phylogeographic and structural dimensions of vegetation and the fuel array (e.g., Pausas and Keeley, 2009; Keeley et al., 2011; Alvarado et al., 2019). For example, fuel-limited biomes like desert or tundra maintain arid conditions that prevent the growth of burnable biomass. Moisture-limited temperate forest systems, on the other hand, experience years- to decades-long lagged growth typical of the classic negative exponential fuel accumulation curve (i.e., Olson, 1963), while the most productive tropical forests tend to retain enough water that they rarely burn (Murphy et al., 2013). For these moisture-limited biome types, fuel moisture plays the key role in whether the landscape can ignite and maintain a wildfire.

## 4.2 Interpreting the ecoregion flammability threshold

The EFT method was applied using global scale data and is therefore an ecological generalization. Although there is variability within each ecoregion due to terrain, vegetation, and fuel structure, EFTs are still biologically meaningful across ecoregions and should be interpreted as *representative* thresholds. That is, when the average DFFMC nears or falls below our identified EFT for a given ecoregion, that reflects an average state of susceptibility across that landscape rather than a strict measure of the moisture content of all fuel particles. It's also important to acknowledge some EFTs are inaccurate or imprecise. Sources of error include the short length of the underlying remotely sensed fire records and the differential importance of fuel moisture as a fire trigger across the productivity gradient (Figure 5a-c). For instance, the modelled  $P(BA < DFFMC)$  relationships for some ecoregions feature gradual shifts in the cumulative proportion of burnt area over the full range of DFFMC (supporting information). In other cases, we identified EFTs well above the upper limits of the fibre saturation point (i.e.,  $> 30\%$ ; Fernandes et al., 2008). Both these cases could reflect a lack of available fire data within that ecoregion, differences in local land-use practices (e.g., savanna or agricultural lands: Le Page et al., 2010; Andela et al., 2017), that the role of fuel moisture for fire ignition and spread in that ecoregion is less important (e.g., Alvarado et al., 2019), or a combination of these factors. Furthermore, the ERA5 grid scale resolution ( $0.25^\circ$ ) may be too coarse to accurately capture and differentiate the climatology of small ecoregions from surrounding regions. This includes most flooded grasslands and savanna and tropical and subtropical coniferous forests given their small size, number, and limited geographic range (supporting information).

Our results show that eco-climatic factors explain a large proportion of the variation in the EFTs amongst the ecoregions (Figure 4a-b, Table 1 and supporting information). Overlaying biome means onto the NMDS ordination, for example, shows that the lowest EFTs in desert environments (Q1: 4.2%; Q3: 8%) are strongly associated with precipitation seasonality and low overall precipitation variables. The highest EFTs in tundra environments (Q1: 17.7%, Q3: 19.8%) are notably associated with high percent herbaceous cover and lower temperatures. Higher-latitude temperate forests – particularly those with higher EFTs like boreal forests (Q1: 13.9%, Q3: 16.6%) and coniferous forests (Q1: 9.3%, Q3: 17.2%) – are associated more strongly with a combination of precipitation, temperature, and seasonality. It is important to note, however, that the precipitation NMDS axis includes the effects of NPP and percent tree cover, which conforms to pyrogeographic theory between productivity and global fire activity (Pausas and Bradstock, 2007; Pausas and Ribeiro, 2013; Jones et al., 2022). For example, low-productivity deserts and xeric shrublands feature the most extreme combination of EFTs, IPSEs, and productivity on Earth (median of  $0.17 \text{ t C ha}^{-1} \text{ year}^{-1}$ ; Figures 5b-c). However, fire activity in these environments is controlled by intermittent periods of high productivity rather than moisture content (Archibald et al., 2009; Bradstock, 2010; Kelley et al., 2019).

The relationship between fire activity, fuel moisture, and fuel availability invites consideration of climate change. Climate change can manifest itself directly (via fuel moisture) and indirectly (via production of phytomass). Those environments with abundant fuel and higher EFTs are often those most vulnerable to climatic change. Tropical and subtropical rainforests, for example, feature high moisture and high fuel and are at risk of catastrophic change, largely driven by human land-use impacts on fire regimes (Le Page et al., 2010; Canadell et al., 2021). Mediterranean forests are among the least productive forests in the world (Figure 5a-c) and could shift towards savanna or desert environment as drying trends continue and leave fuel accumulation unable to keep up with increasing fire intensity (Pausas and Paula, 2012; Pausas and Bond, 2020). The most arid desert landscapes rarely support enough fuel for fire spread (Bradstock, 2010; Murphy et al., 2013; Bedia et al., 2015), and are unlikely to have fire regimes driven by anthropogenic climate change except along biome transition lines (Archibald et al., 2009; Senande-Rivera et al., 2022). At the upper limits of the intermediate fire-productivity zone, the most important intersection supports higher productivity ( $> 4.5 \text{ t C ha}^{-1} \text{ year}^{-1}$ ), higher fire activity ( $> 0.5 \text{ FAI}$ ), and extreme values of both EFT and IPSE (Figures 5b-c). This area reflects some of the most at-risk environments under climatic change, including many higher-latitude temperate broadleaf and boreal forests susceptible to ecological collapse under drying climate trends (Ellis et al., 2022; Senande-Rivera et al., 2022), as well as more productive, moisture-limited tropical savanna ecoregions (e.g., Alvarado et al., 2019).

One important advance our identified EFTs provide is the elimination of the persistent uncertainty in defining fire season onset – a key pyrogeographic parameter that further defines fire regimes and pyromes. At the continental scale, for example, Australia’s fire-prone tropical and temperate ecoregions feature fire season onsets driven by a distinct latitudinal climate gradient (Murphy et al., 2013; Williamson et al., 2016). The evident drying trend in fuel moisture for wet *Eucalyptus* forests along this gradient places those ecoregions at risk of a potential collapse due to increasing fire frequency (Bowman et al., 2014; Furlaud et al., 2021; McColl-Gausden et al., 2022). Worldwide, boreal forests, Mediterranean forests, and both temperate and tropical broadleaf and coniferous forests are all at risk due to increasing burnt area, fire frequency or both (Westerling, 2016; Forkel et al., 2019; Kelley et al., 2019; Abatzoglou et al., 2021; Ellis et al., 2022). Our EFTs can be used to detect the onset of a fire season in real time in environments like these, which is of primary importance to tracking the effects of climate change on different landscapes’ fire activity, as well as determining the allocation of forest management and firefighting resources.

Specific EFTs will be useful in understanding changes in fire seasons for individual ecoregions, biomes, and specific vegetation types globally. The identification of changing length, intensity, and extremes of fire seasons using meteorological data has been an important line of evidence of changing global fire risk. However, previous analyses have used generalised or assumed thresholds to which this study provides a key innovation. Additionally, the expansion of the active fire season is not just occurring at the seasonal boundaries, but into the night-time – a period previously assumed to provide relief from rapid wildfire spread (Balch, et al., 2022). To advance our understanding of shifting fire regimes under anthropogenic stressors, identifying the biogeography of EFTs as we have done is a prerequisite for defining the bounds of the fire seasons, as well as conducting trend analyses sensibly informed by the local fuel-fire relationship. Such trend analyses can be used to identify and manage those most at-risk environments for ecological collapse under predicted future fire regimes.

## 5 Conclusion

Bridging local meteorological conditions, vegetation, and anthropogenic influences to understand fine-scale fire regimes, our identification of ecoregion flammability thresholds (EFTs) is an essential step in providing managers and researchers a way to monitor the ongoing shifts in local fire regimes, as well as anticipate changing fire seasonality. Our results also highlight precipitation, temperature, and seasonality as important climatic drivers of EFTs, providing insight into how those critical thresholds and their association with the local environment can further shift under anticipated widespread drying trends. Additionally, our analyses further highlight regional variability in the role fuel moisture plays with fire – that, for example, an assumed threshold of between 8 and 12% commonly used in prior research does not work for all temperate coniferous forests (Figures 2a, 3). We present a dataset of 772 identified EFTs representing critical thresholds with fire for much of the Earth’s terrestrial surface. Additionally, we identify the inflection point slope estimate (IPSE), an essential component in interpreting the EFT as a driver of wildfire. These global data can and should be used as a steppingstone for understanding and managing fire regimes at the ecoregion level under continued anthropogenic climate change and constantly evolving land-use practices. Identifying the critical EFT as we have done therefore provides an important stage for future wildfire research.

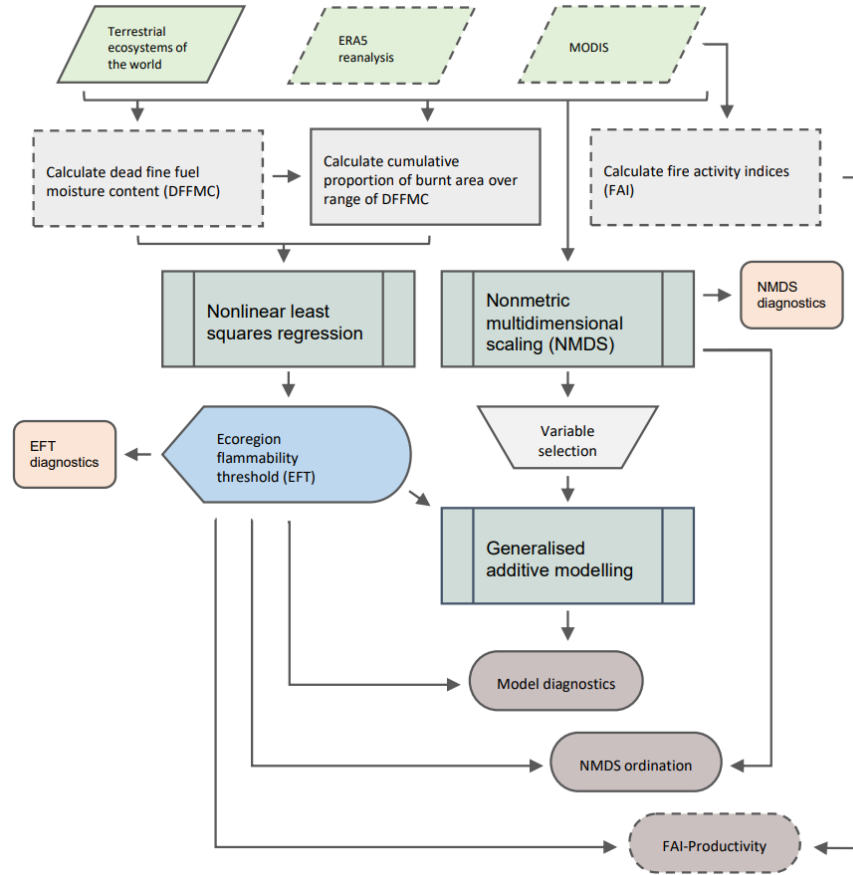


Figure 1: Workflow diagram showing our data sources, applied methods, and outputs. Dashed outlines represent  $0.25^\circ$  gridded data or analyses performed at the  $0.25^\circ$  grid cell level, while solid outlines represent data or analyses summarised at the ecoregion level. ERA5 reanalysis data include daily meteorological timeseries (Hersbach et al. 2020) as well as bioclimatic indicator means (BIO01, BIO12, and BIO15: Wouters et al., 2021). MODIS products include MCD64CMQ (Giglio et al., 2018), MOD17A3 (Running et al. 2015), MOD44B (DiMiceli et al., 2015), and MCD14DL (Giglio et al., 2003). Output products include model diagnostics (Table 1 and additional supporting information), visualised NMDS ordination (Figure 4), and the FAI-productivity analysis (Figure 5).

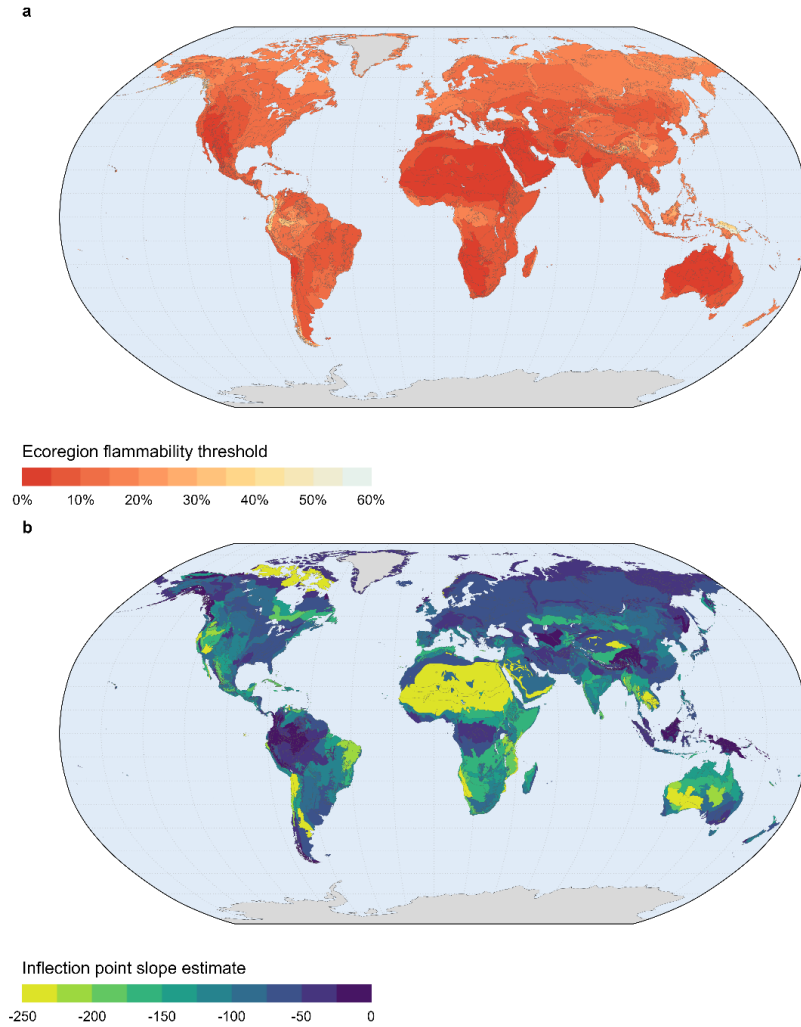


Figure 2: Map showing the global distributions of a) identified ecoregion flammability thresholds (EFTs) and b) the associated inflection point slope estimates (IPSEs) extracted from the  $P(BA < DFFMC)$  models' scaling parameter. For IPSEs, lower values represent stronger negative associations between cumulative burnt area probability and DFFMC. Note that displayed EFTs and IPSEs include imputed values.

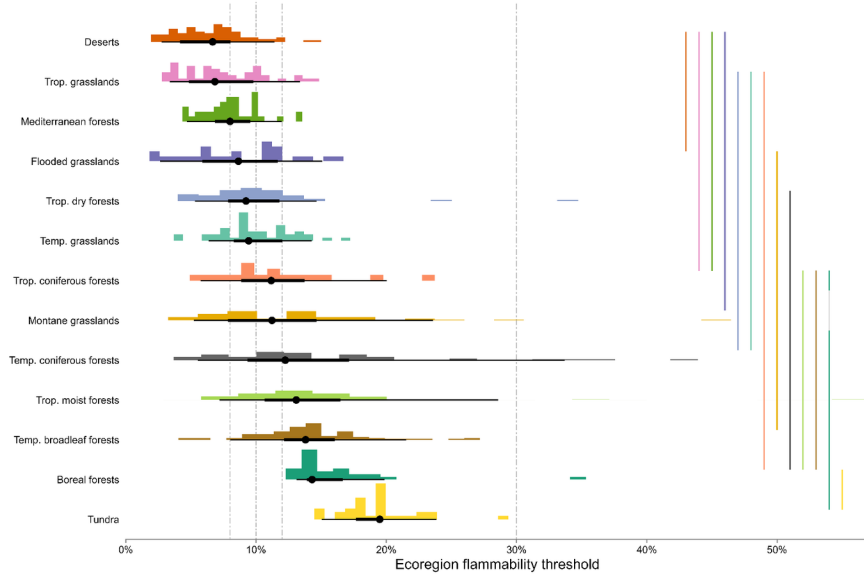


Figure 3. Distributions of the identified ecoregion flammability thresholds (EFTs) by biome type and ordered by median EFT. Point and line intervals under histograms represent the median equal-tailed distribution intervals of 50 and 90%. Dashed vertical lines reference EFT values (8, 10, 12, and 30%) identified as important biophysical thresholds constraining fire ignition and spread in prior research (Boer et al., 2017; Fernandes et al., 2008; Filkov et al., 2019; Flannigan et al., 2016; Nolan et al., 2016; Wotton, 2008). Vertical lines and dots on the right reflect non-significant differences in Dunn's Z statistics for pairwise multiple comparisons: E.g., the mean rank value of EFTs for deserts and xeric shrublands is comparable to the three biome types below it. Note that boreal forests and taiga features a break in statistical significance: It is statistically significantly different from montane grasslands and savannas, but not tropical and subtropical coniferous forests.

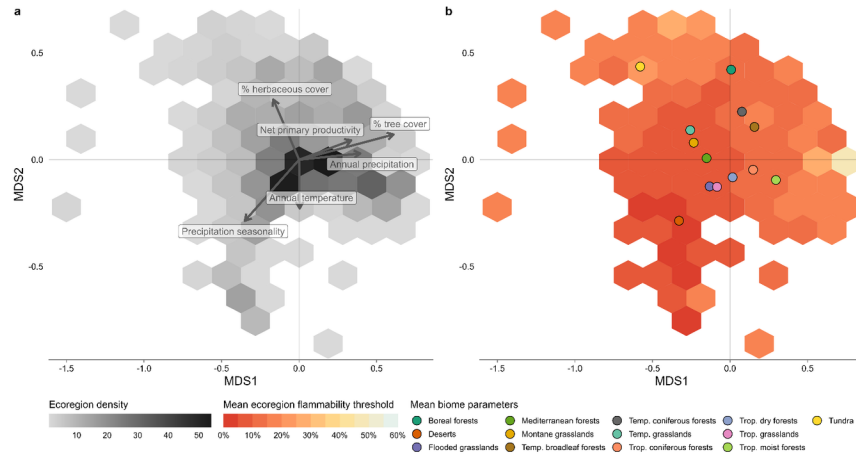
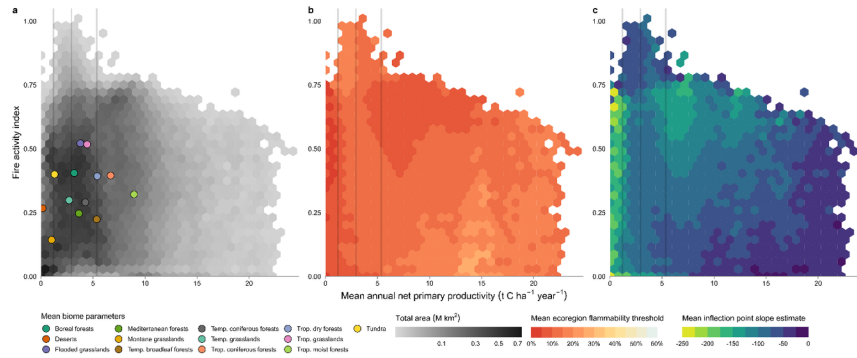


Figure 4: First and second dimensions produced by our application of nonmetric multidimensional scaling (NMDS) using eco-climatological variables holding established associations with wildfire ignition or spread. Figure includes both the a) density distribution of the underlying ecoregions represented in the analyses with arrows representing the strength and direction of variable influence within the new multidimensional scaled dimensions; and b) the median underlying ecoregion flammability threshold (EFT) binned using those values

(8, 12, and 30%) identified as important biophysical thresholds constraining fire ignition and spread in prior research (Boer et al., 2017; Fernandes et al., 2008; Filkov et al., 2019; Flannigan et al., 2016; Nolan et al., 2016; Wotton, 2008) as well as points representing the biome-level mean MDS1 and MDS2 values.



**Figure 5:** Adaptation of the intermediate productivity-fire activity hypothesis as drawn from Ellis et al. (2022) using a) the total underlying represented area ( $M \text{ km}^2$ ) of the Earth’s surface, b) the mean underlying ecoregion flammability threshold (EFT) and c) the mean underlying inflection point slope estimate (i.e.,  $1 / \beta_3$ ). Solid vertical lines in all figures highlight the 25<sup>th</sup>, 50<sup>th</sup>, and 75<sup>th</sup> percentiles of global net primary productivity (NPP) for all ecoregions with identified EFTs, roughly illustrating the range of intermediate productivity most associated with fire activity ( $\sim 1.2 - 5.4 \text{ t C ha}^{-1} \text{ year}^{-1}$ ); points in c) represent the mean location for biome-level NPP and fire activity indices, highlight that most ecoregions are, if not within the intermediate productivity range, near it.

Parameter	Parameter type	Median	89% HDI	Existence	Significance	Size
Mean annual precipitation	Non-linear ( $k = 5$ )	3.451	[2.294, 4.575]	100.0%	100.0%	100.0%
Mean precipitation seasonality	Non-linear ( $k = 8$ )	-1.337	[-2.183, -0.669]	99.9%	99.7%	99.4%
Mean annual temperature	Non-linear ( $k = 5$ )	1.176	[0.400, 1.922]	98.8%	97.3%	96.1%
Median % herbaceous cover	Linear	-0.126	[-0.259, 0.006]	93.3%	26.0%	1.9%

Table 1: Descriptive statistics for continuous linear and non-linear model parameters. Includes the median of the posterior predictive distribution, the 89% highest density interval (HDI), and probabilities of effect existence, significance, and size. Model significance scoring is based on an estimated ROPE value of 0.181 and the size estimate is based on a default recommended value of 0.3 based on exploratory analysis.